The 2010 IEEE/RSJ International Conference on
Intelligent Robots and Systems
October 18-22, 2010, Taipei, Taiwan

Human force amplification with industrial robot : study of dynamic limitations

Xavier Lamy[1], Frédéric Collédani[1], Franck Geffard[1], Yvan Measson[1], Guillaume Morel[2]
[1]CEA, LIST, Interactive Robotics Laboratory, Fontenay aux Roses, F- 92265, France firstname.lastname@cea.fr
[2]University of Paris6-UPMC, Insitut des Systèmes Intelligents et de Robotique (CNRS - FRE 2507) morel@robot.jussieu.fr

Abstract— **In the field of comanipulation (i.e. a man and a robot sharing the same task), force amplification is an interesting function that can be achieved by using two force sensors. This technique is known in the literature but little attention has been paid so far to stability/passivity properties. We will explain how to deal with passivity based stability criteria, and point out performance limitations of such a control in case of noncollocated and bandwidth limited force sensors. Theoretical, as well as experimental results will be presented.**

I. Introduction

The domain of cobotics covers systems involving a human operator and a robot working in the same operating space, sharing the same task, and thus interacting physically. This area (also called comanipulation) is growing fast, since it gives the opportunity to mix advantages of a human worker and industrial robots.

Unlike many other papers describing human interactions with dedicated robots, mechanically designed to take into account man−robot interactions, our work focuses on the developments needed to make man−industrial robots interactions efficient and safe.

There are many reasons why the interaction of a human operator and an industrial robot are relevant. Industrial robots have been design to optimize strength, velocity, precision and stiffness. This is why they are commonly used for medium or large series manufacturing. On the other hand, human workers are able to rapidly learn complex tasks. They better understand environment changes and task status, with great adaptation skills. That is why human workers are still preferred for manipulation tasks that are repeated less times, or for tasks that may differ a little bit each time. Thanks to this complementarity between industrial robots and human skills, comanipulation can be applied to optimize ergonomy, to limit efforts, to increase precision, to secure the task, ...

The basic function to be implemented in most applications is force amplification: the operator applies some force to the robot, and the robot applies 10 times this force to the environment. This will allow the operator to guide the robot, using it strength to perform the task with much less effort. The fact that the operator input is a force allows to get direct feedback, enabling him to better understand his action. With a position input, the robot would use an abitrary saturated force on the environment to follow the position set-point, increasing the risk of applying unwanted force on the environment. Various other functions such as gesture guidance, tremor filtering, etc., can also be useful and are worth implementing.

Among the historical papers focusing on the use of robots as a collaborative assistant to human workers, we can cite [1], [2], [3]. In such cooperation, the operator and the robotic system share the same workspace. A major issue is thus to ensure the user safety while operating the robot. This issue may be addressed for example using a robotic skin [4].

However, although the basic principles of comanipulation are well known, there are still a lot of theoretical aspects that need to be addressed for efficient and easy-to-use cobotics, and these aspects are not commonly seen in the literature. For example, estimating the performances of such a system was never really considered. Different aspects have to be taken into account: operator fatigue or lack of precision of the task can be due to apparent inertia, apparent friction, or lack of ability to easily change effort direction, ...

The main contribution of this paper is to point out performance limitations of force amplification controllers, that were never theoreticaly and experimentally discussed before.

This paper is organized as follows: first of all, the choice of sensors location will be discussed. Then we will present a practical way of modeling the robot flexibility to ensure that the developed control will be efficient and remains stable in contact with any environnement. The chosen control algorithm will then be presented, and their stability discussed. Then various issues in dynamic behavior of the robot will be raised, from the contact establishment situation, to the minimization of robot apparent inertia.

II. Problem of interest

Let us focus on the application example described on Fig. 1: an operator needs to cut slices of ham with the help of the robot. The system consists of the robot, a handle and a separate blade connected at the robot end-effector with a setup similar to a classical knife. We want to control the robot such as the force applied by the blade to the ham is 10 times the force applied by the human operator to the handle. This implies that, at equilibrium, the robot has to provide to the blade 9 times the force applied by the operator to the handle.

A. Sensor relative positioning

In order to achieve such a control task, we need to obtain an estimation of both forces. If the robot is non- or

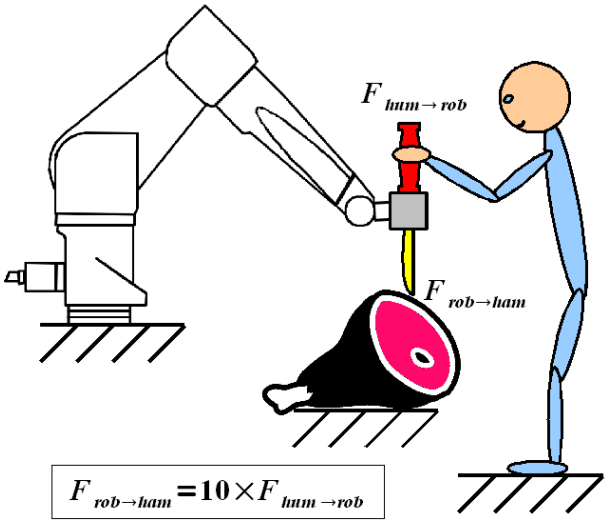

Fig. 1. This picture represents a typical configuration of an industrial robot used as a human force amplification system. In this example the robot is controlled such as the force applied by the blade to the ham is 10 times the force applied by the human operator to the robot handle.

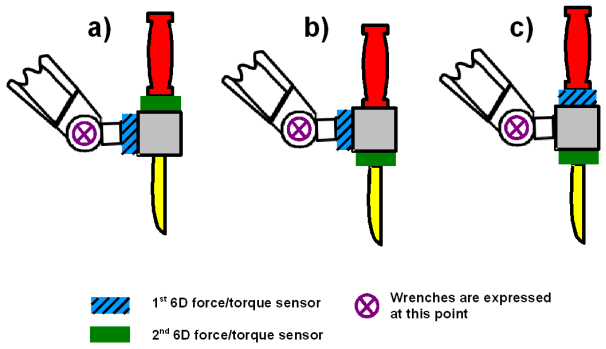

Fig. 2. There are three possible configurations for the force/torque sensors localization, but a) and c) best suit operator force amplification. On our experimental setup, we implemented the localization a).

poorly backdrivable, as most industrial robots are, because of the usual high ratio transmission gears in the actuation mechanism, we need to use two 6D force/torque (F/T) sensors. F/T sensor localization should be chosen to suit the comanipulation task. 3 kind of sensor localizations are possible (see fig. 2).

In our case of operator force amplification, with the configuration a), the operator sensor should be able to measure precisely small values and would be a small range sensor, while the second sensor would measure large forces applied to the tool, and should be chosen of a higher range. This is not possible with the localization b), because the operator intention is measured by difference of the 2 F/T sensors. Consequently, the 2 sensors would have to be in the tool force range, thus restricting the precision on the operator force measurement.

On the contrary, and for symmetrical reasons, localization b) suits best the amplification of the tool force sensed by the operator (eg. a surgeon doing fine operation). In that case, the tool sensor would be a very precise low range sensor, while the global sensor would have the operator range.

Localization c) may be used for both cases. In some application, it may have the drawback to leave a larger distance between the tool and the handle.

If articular torque measurement is available (in case of robots with high backdrivability performances such as haptic interfaces or in case of robots with an articular built-in torque sensor such as the Kuka-DLR LWR3), then only one FT sensor is needed, because articular torques are transposable to the 1st FT sensor of localisation a) or b).

On our experimental setup, we implemented localization a), since we study operator force amplification.

B. Proposed Control

The proposed control on fig.4 is inspired from classical impedance control such as NAC proposed by [5] and the force amplifier from [6]. In the context of this study, we will only consider a 1 DoF problem: only the first axis of the robot will be controlled, while the other axes will be kept fixed thanks to high stiffness joint position controllers and singular configuration (see fig. 3).

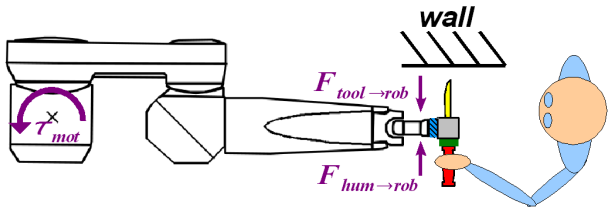

Fig. 3. Only the first axis of the robot will be controlled, whereas the other axes will be kept fixed thanks to high stiffness joint position controllers and singular configuration.

$J \in \mathbb{R}^{6\times 1}$ stands for the Jacobian matrix of the resulting 1 DoF robot. The force/torque (wrench) exerted by the human operator on the end-effector handle is represented by the column vector $\mathbf{F}_{\text{rob}\rightarrow\text{hum}} \in \mathbb{R}^{\mathbf{6}}$. The projection of this wrench on the first joint of our robot is $f_h \in \mathbb{R}$. Similarly, we define $\mathbf{F}_{\text{rob}\rightarrow\text{tool}} \in \mathbb{R}^{\mathbf{6}}$ the wrench exerced by the tool and its workload environement on the end-effector of the robot and $f_t \in \mathbb{R}^6$ its projection in the joint space. We also define $\mathbf{V}_{\text{rob}} \in \mathbb{R}^6$ the end-effector velocity (twist) of the robot and v_{r} its projection on the joint. Jacobian and wrenches are expressed at the center of the robot wrist in order to simplify their formulation. We have the following relationship:

$$f_h = J^T . \mathbf{F}_{\text{rob}\rightarrow\text{hum}} \quad (1)$$

$$f_t = J^T . \mathbf{F}_{\text{rob}\rightarrow\text{hum}} \quad (2)$$

$$v_{\text{r}} = J^{-1} . \mathbf{V}_{\text{rob}} \quad (3)$$

We will assume that the velocity controlled robot can be described by a linear model. As shown on fig. 4, this linear model would be composed by two transfer functions $\alpha(s)$ and $\beta(s)$ as done in [7]. $\alpha(s)$ represents the transfer function

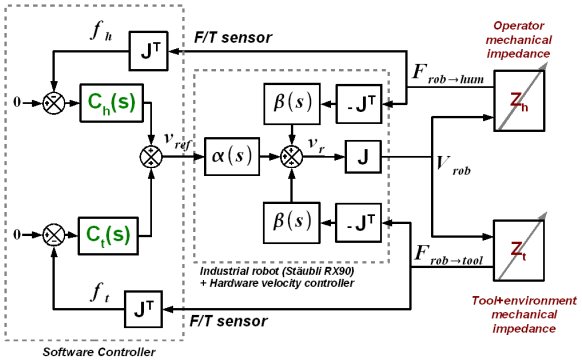

Fig. 4. The force amplification controller scheme, connected to our robot model with operator and tool impedances.

of the velocity command to the robot end-effector velocity when it is moving freely. $\beta(s)$ represents the admittance of the robot end-effector when $v_{ref} = 0$. This representation may include modeling of the robot flexibilities as well as sensor bandwidth limitations that were not taken into account in the study of [6].

$$\alpha(s) = \left.\frac{\partial v_r}{\partial v_{ref}}\right|_{f_h = f_t = 0} \quad (4)$$

$$\beta(s) = -\left.\frac{\partial v_r}{\partial (f_h + f_t)}\right|_{v_{ref} = 0} \quad (5)$$

Our controller will be composed of two force error compensator, $C_h(s)$ and $C_t(s)$, that will output velocity commands that will be summed up to form the input to the motor velocity controller, v_{ref}. Note that the purpose of using the proportional velocity controller is mainly to reduce the non-linear effects of friction as done in Natural Admittance Control (NAC) [5]. We then define $0 \leq 1/\gamma \leq 1$ the force amplification factor. For example if we want the force applied to the tool to be 10 times the force applied by the operator on the handle, we will choose $\gamma = 1/10$. If we assume those controller have at least one integrator, then to achieve our goal we only need to have :

$$\lim_{s \to 0} \frac{C_t(s)}{C_h(s)} = \gamma \quad (6)$$

C. Simple Non-collocated sensor model

As our control implements an extension of a classical impedance controller, we expect that the non-collocation of the force measurement and the robot actuation will limit the achievable gains and performance. Thus we will model the dynamics of the robot as described in fig. 5 with two separate inertias: J_m for the motor side, and J_r for the effector side. Those inertias are connected together with a transmission stiffness K_t and damping B_t. B_m is the viscous friction at the motor level. q_m is the position of the motor side inertia

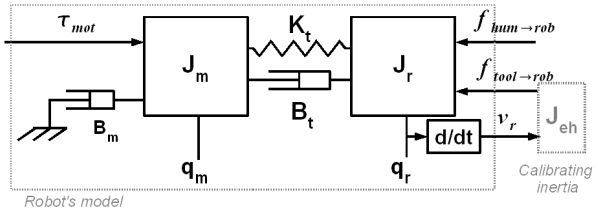

Fig. 5. Model of the non-collocation of the actuator and the force sensors.

and q_r the position of end-effector side inertia expressed in the articular domain. The following equations describe our model:

$$q_m.s^2.J_m = \tau_{mot} + (K_t + s.B_t).(q_r - q_m) - B_m.s.q_m \quad (7)$$

$$q_r.s^2.J_r = (K_t + s.B_t).(q_m - q_r) + f_h + f_t \quad (8)$$

In order to identify J_r, K_t and B_t of fig. 5, we have rigidly connected a known heavy mass $J_{e_h} = 13.5\ kg.m^2$ to the end-effector after the first F/T sensor, instead of the regular tool and handle of fig. 2a). Then we excited the robot at each frequency from 1 Hz to 100 Hz and recorded the response of q_m and f_t. The transfer function H_v from v_m to v_r is obtained with:

$$v_m(s) = q_m(s).s \quad (9)$$

$$v_r(s) = \frac{f_t(s)}{s.J_{e_h}} \quad (10)$$

$$H_v(s) = \frac{v_r(s)}{v_m(s)} = \frac{K_t + s.B_t}{K_t + s.B_t + s^2.(J_r + J_{e_h})} \quad (11)$$

It is important to notice that J_m and B_m do not appear in the expression of H_v. If B_t is too low, parameters K_t and J_r are not identifiable separately. Thus the same experiment is reconducted replacing J_{e_h} with a known lower inertia $J_{e_l} = 3.31\ kg.m^2$, then we used an optimization algorithm to identify the best fitting parameters B_t, K_t and J_r common to both experimental results. In fig. 6, we show the result of our identification process compared to the heavy inertia experiment.

Using the response at 1 Hz of the transfer function from τ_{mot} to q_m allows identification of J_{tot} the global inertia projected on the articulation and B_m, with enough accuracy. J_m can then be calculated with:

$$J_m = J_{tot} - J_r - J_{e_l} \quad (12)$$

After this identification process we found the following numerical value for our model parameters :

$$\begin{array}{lcll} J_r & = & 13.9 & kg.m^2.rad^{-1} \\ K_t & = & 6.72e4 & N.m.rad^{-1} \\ B_t & = & 48.7 & N.m.rad^{-1}.s \\ J_m & = & 8.5 & kg.m^2.rad^{-1} \\ B_m & = & 132 & N.m.rad^{-1}.s \end{array}$$

We can also model the hardware velocity controller with the following equation,

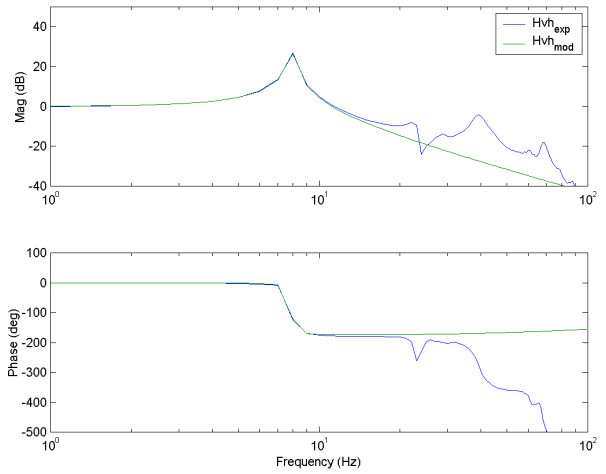

Fig. 6. Experimental result of the non-collocation transfer function $H_{v_{exp}}$: response of the robot end-effector velocity to robot motor velocity excitation. The identified model is $H_{v_{mod}}$

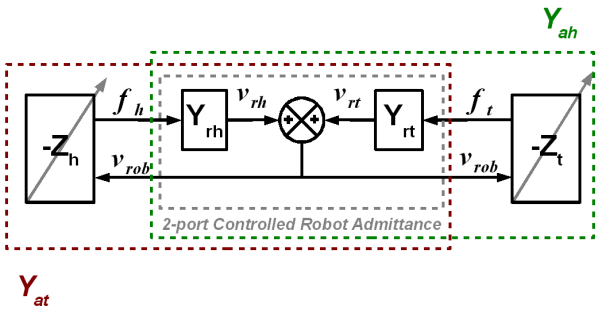

Fig. 7. The controlled robot system may be represented as a 2-port system composed by the two independent admittances of the controlled robot Y_{rh} and Y_{rt}

$$\tau_{mot} = K_v.(\frac{v_{ref}}{1+s.T_c} - \frac{q_m.s}{1+s.T_{cv}}) \quad (13)$$

where K_v is the proportional gain, T_{cv} represents the motor velocity measurement bandwitdh limitation. It is also convenient to introduce here T_c, the force sensor bandwidth limitation. On our hardware, we have the following numerical values :

$$\begin{array}{lcll} K_v & = & 710 & N.m.rad^{-1}.s \\ T_c & = & 1.59e{-}3 & rad^{-1}.s \quad (bw = 100Hz) \\ T_cv & = & 3.98e{-}3 & rad^{-1}.s \quad (bw = 40Hz) \end{array}$$

For simplicity we express here $\alpha(s)$ and $\beta(s)$ without considering bandwidth limitation ($T_c = 0$, $T_{cv} = 0$). Using equations 7, 8 and 13 we obtain :

$$\alpha(s) = \frac{(B_t.s + K_t).K_v}{den} \quad (14)$$

$$\beta(s) = \frac{J_m.s^2 + (K_v + B_t + B_m).s + K_t}{den} \quad (15)$$

$$\begin{aligned} den = {} & J_r.J_m.s^3 + (J_r.K_v + B_t.J_m + (B_t + B_m).J_r).s^2 \\ & + (B_t.K_v + (J_m + J_r).K_t + B_m.B_t).s + K_t.K_v + B_m.K_t \end{aligned} \quad (16)$$

III. Stability criteria

A. Two port admittance representation

Refering to teleoperation one may see our system as a particular master-slave setup, where the both mechanical interaction ports are put on the same robot. The main difference is that the two ports share exactly the same velocity v_r. It will be useful to translate our system into the 2-port admittance representation of fig. 7.

In fig. 7, Y_{rh} is the robot admittance at the operator interaction port (the handle) when no force is applied on the tool port, and Y_{ah} is the global admittance appearing to the operator when the tool port is used. Symetrically Y_{rt} is the robot admittance at the tool interaction port when no force is applied on the operator port, and Y_{at} is the global admittance appearing to the tool when the operator port is connected.

$$Y_{\mathrm{rh}}(s) = -\left.\frac{\partial v_{\mathrm{r}}}{\partial f_h}\right|_{f_t=0} = \alpha.C_h + \beta \quad (17)$$

$$Y_{\mathrm{rt}}(s) = -\left.\frac{\partial v_{\mathrm{r}}}{\partial f_t}\right|_{f_h=0} = \alpha.C_t + \beta \quad (18)$$

$$Y_{\mathrm{ah}}(s) = -\frac{\partial v_{\mathrm{r}}}{\partial f_h} = \frac{Y_{rh}}{1 + Z_t.Y_{rt}} \quad (19)$$

$$Y_{\mathrm{at}}(s) = -\frac{\partial v_{\mathrm{r}}}{\partial f_t} = \frac{Y_{rt}}{1 + Z_h.Y_{rh}} \quad (20)$$

B. Passivity considerations

It is well known that a passive system is stable (in Lyapunov sense) when connected to any other passive environments [8] and that a human operator can be considered as a passive environment with varying impedance Z_h [9]. In our example of meat cutting, the knife, since it can be in contact with the ham or the table, or without any contacts, can also be considered as an extremely varying impedance Z_t. However Z_t always stays inside the passivity bounds.

A linear 1-port system with admittance/impedance $X(s)$ is passive iff [8]:

- $X(s)$ has no poles in the right half plane. (21)
- any imaginary poles of $X(s)$ are simple, and have positive real residues. (22)
- $\Re(X(\mathbf{j}\omega)) \geq 0,\ \forall \omega \in \mathbb{R}^+$ (23)

As we will see in this article the corrector gains are mostly constrained by the third condition (23). So in the following it will be useful to split previously defined admittance/impedance in real and imaginary part denoted by a and b respectively, in order to particulary check this condition:

$$Z_t(\mathbf{j}\omega) = \quad aZ_t(\omega) + \mathbf{j}.bZ_t(\omega), \quad aZ_t \geq 0 \ \forall \omega \in \mathbb{R}^+ \quad (24)$$

$$Z_h(\mathbf{j}\omega) = \quad aZ_h(\omega) + \mathbf{j}.bZ_h(\omega), \quad aZ_h \geq 0 \ \forall \omega \in \mathbb{R}^+ \quad (25)$$

$$Y_{rt}(\mathbf{j}\omega) = \quad aY_{rt}(\omega) + \mathbf{j}.bY_{rt}(\omega) \quad (26)$$

$$Y_{rh}(\mathbf{j}\omega) = \quad aY_{rh}(\omega) + \mathbf{j}.bY_{rh}(\omega) \quad (27)$$

C. Unconditionnal Coupled Stability

Restricting our system to be 2-port passive doesn't make sense in our case: force amplification through ports that share the same velocity requires an active behaviour from the robot.

Therefore we will focus on a less restrictive stability criteria that is used in telerobotics: Unconditionnal Coupled Stability criteria (UCS). The assumption made for this criteria is that operator and tool only exchange energy through the robotic system. While this assumption is easily verified in telerobotics, in commanipulation this mainly restricts the operator to not grasp the tool with its other hand to insure stability with such a system. A system satisfies the UCS criteria iff:

$$\begin{cases} Y_{ah}(Z_t) & is\ passive, \quad \forall Z_t\ passive \\ Y_{at}(Z_h) & is\ passive, \quad \forall Z_h\ passive \end{cases} \quad (28)$$

Substituting (20) and (19) in the condition (23) of passivity definition necessary to (28), we obtain the following necessary conditions for UCS, $\forall \omega \in \mathbb{R}^+$:

$$(aY_{rt}.aY_{rh} + bY_{rh}.bY_{rt}).aZ_t + (aY_{rt}.bY_{rh} - aY_{rh}.bY_{rt}).bZ_t + aY_{rh} \geq 0 \quad (29)$$

$$(aY_{rt}.aY_{rh} + bY_{rh}.bY_{rt}).aZ_t + (aY_{rt}.bY_{rh} - aY_{rh}.bY_{rt}).bZ_t + aY_{rh} \geq 0 \quad (30)$$

Given the passivity condition on Z_t and Z_h (24 and 25), this is equivalent to meeting the following necessary conditions, $\forall \omega \in \mathbb{R}^+$:

$$aY_{rh} \geq 0 \quad (31)$$

$$aY_{rt} \geq 0 \quad (32)$$

$$aY_{rh}.aY_{rt} + bY_{rh}.bY_{rt} \geq 0 \quad (33)$$

$$aY_{rt}.bY_{rh} = aY_{rh}.bY_{rt} \quad (34)$$

It seems difficult to fullfill condition (34). In fact (31), (32) and (34) imply that :

$$Y_{rt}(\mathbf{j}\omega) = \gamma(\omega).Y_{rh}(\mathbf{j}\omega), \ \gamma(\omega) \in \mathbb{R}^+ \quad (35)$$

Using (17) and (18) in (35) lead to the following necessary condition for UCS :

$$C_t(\mathbf{j}\omega) = \frac{\beta(\mathbf{j}\omega)}{\alpha(\mathbf{j}\omega)}(\gamma(\omega) - 1) + \gamma(\omega).C_h(\mathbf{j}\omega) \quad (36)$$

Unfortunatly for Non-Collocated sensor feedback such as in fig. 5, $\frac{\beta(\mathbf{j}\omega)}{\alpha(\mathbf{j}\omega)}$ has more zeros than poles. This means that $C_t(s)$ need to be a non-causal corrector. Thus UCS on a force augmentation robot is not achievable.

D. Unconditionnal Coupled Stability with limited tool inertia

We need to introduce a weaker stability criteria that will essentially relax cond. 34. Consider that the tool impedance connected to the robot could be modelised by a mass+spring+damper mechanical system as shown on fig. 8 .Its impedance would be :

$$Z_t(s) = J_{tool}.s + B_{tool} + \frac{K_{tool}}{s} \quad (37)$$

$$\Rightarrow \begin{cases} aZ_t(\omega) = B_{tool} \\ bZ_t(\omega) = J_{tool}.\omega - \frac{K_{tool}}{\omega} \end{cases} \quad (38)$$

This may represent as well a tool moving freely unconstrained ($B_{tool} = K_{tool} = 0$) or tool in contact with stiff environment (high K_{tool}).

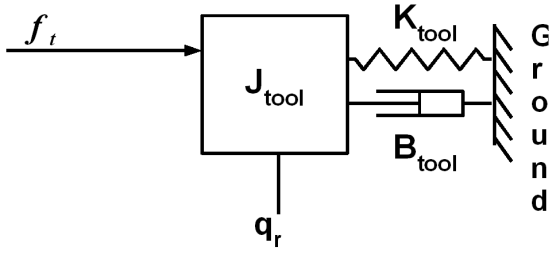

Fig. 8. The tool impedance model

If we restrict the inertia of the tool that the robot is allowed to bear, to be less than J_{tmax} then it is possible to modify the UCS criteria to the weaker one taking into account that bZ_t is upper bounded. A system satisfies the UCS with limited tool inertia iff:

$$Y_{ah}(Z_t)\ is\ passive, \ \forall Z_t \begin{cases} passive \\ \Im(Z_t(\mathbf{j}\omega)) \leq J_{tmax}.\omega \end{cases} \quad (39)$$

As previously, substituting (19) in the condition (23) of passivity definition necessary to (39), we obtain the following necessary conditions for UCS with limited tool inertia, $\forall \omega \in \mathbb{R}^+$:

$$(aY_{rt}.aY_{rh} + bY_{rh}.bY_{rt}).aZ_t + (aY_{rt}.bY_{rh} - aY_{rh}.bY_{rt}).bZ_t + aY_{rh} \geq 0 \ , \ \forall \begin{cases} aZ_t(\omega) \geq 0 \\ bZ_t(\omega) \leq J_{tmax}.\omega \end{cases} \quad (40)$$

That is equivalent to meet the following necessary conditions:

$$aY_{rh} \geq 0 \quad (41)$$

$$bY_{rh}.bY_{rt} + bY_{rh}.bY_{rt} \geq 0 \quad (42)$$

$$aY_{rt}.bY_{rh} - aY_{rh}.bY_{rt} \leq 0 \quad (43)$$

$$(aY_{rt}.bY_{rh} - aY_{rh}.bY_{rt}).J_{tmax}.\omega + aY_{rh} \geq 0 \quad (44)$$

E. Unconditionnal Coupled Stability with limited tool inertia and stiffness

It is also possible to use a less restrictive stability criteria that would restrict the tool stiffness to be less than K_{tmax}, this could be achieved by inserting for example a compliant part between the robot and the tool:

$$bZ_t(\omega) \geq -\frac{K_{tmax}}{\omega} \tag{45}$$

The necessary conditions for the UCS with limited tool inertia and stiffness would be the same as UCS with limited inertia, but (43) is replaced by:

$$(aY_{rt}.bY_{rh} - aY_{rh}.bY_{rt}).\frac{-K_{tmax}}{\omega} + aY_{rh} \geq 0 \tag{46}$$

IV. Application to the flexible robot model

We will now apply the UCS with limited inertia criteria to our simple non-collocated sensor robot model. In order to illustrate our method within limited space, we will use the simplified flexible robot model (14) and (15) with $B_t = T_c = T_{cv} = 0$. In the last part of the paper, numerical results with full model will be presented to consider more realistic conditions.

A. Choice of the correctors C_h and C_t

In NAC [5], when we want the robot to emulate a pure inertia behaviour, the force error corrector that is suggested is a PI. Therefore we will restrain our study to a PI structure for both correctors C_h and C_t. In order to satisfy (6) we need to have linked integrator gains:

$$C_h(s) = \frac{K_{ih}}{s} + K_{ph} \tag{47}$$

$$C_t(s) = \frac{K_{it}}{s} + K_{pt} \tag{48}$$

$$\text{with } K_{ih} = \frac{K_{it}}{\gamma_0} = K_i \tag{49}$$

B. First and second passivity conditions

Here we will check conditions of passivity (21) and (22) for admittances Y_{rh}, Y_{rt} and Y_{ah}.

$$Y_{rh} = \frac{s^3 + \frac{K_v+B_m}{J_m}.s^2 + \frac{K_{ph}.K_v+1}{J_m}.K_t.s + \frac{K_i.K_t.K_v}{J_m}}{s.(J_r.s^3 + \frac{K_v+B_m}{J_m}.J_r.s^2 + \frac{J_m+J_r}{J_m}.K_t.s + \frac{K_v+B_m}{J_m}.K_t)} \tag{50}$$

All poles of Y_{rh} are independant of the controller gains. There is one simple pole at the origin and we numerically checked that the other were on the half-left plan, excluding the imaginary axis. Thus condition (21) of passivity for Y_{rh} is always true. The residue of the simple pole at origin is :

$$\lim_{s\to 0} s.Y_{rh}(s) = \frac{K_i.K_v}{K_v + B_m} \tag{51}$$

Thus condition of passivity (22) for Y_{rh} is checked iff $Ki \geq 0$. The same consideration could be done for Y_{rt}.

Since connecting two one-port passive system together lead to a Lyapunov-stable closed loop system:

$$\frac{1}{1 + Y_{rt}.Z_t} \text{ is Lyapunov-stable} \tag{52}$$

Therefore (52) also satisfies (21) and (22).
Since Y_{ah} is the product of Y_{rh} with (52), this means that Y_{ah} satisfies (21). Furthermore, the only pole of Y_{rh} on the imaginary axis is at 0. Therefore to satisfy (22) we only need to check that (52) doesn't have also a pole at 0, to avoid having a double pole. This can be demonstrated as follow :
Three cases have to be considered :

a) If Z_t has a zero at 0, it is simple and with positive inverse residue ($\lim_{s\to 0} \frac{Z_t}{s} > 0$), this is due to the fact that since Z_t is passive, then $\frac{1}{Z_t}$ is also passive. Since Y_{rt} has a positive residue at 0 then $\lim_{s\to 0} 1 + Y_{rt}(s).Z_t(s) > 1$, this means that 0 is not a pole of (52).

b) If $Z_t(0) \neq 0$ is defined, we have $\Re(Z_t(0)) > 0$, then 0 is a zero of (52) (thus not a pole).

c) If Z_t has a pole at 0, it is with positive residue, because Z_t is passive. Since Y_{rt} also has a pole at 0 with positive residue, then 0 is a double zero of (52) (thus not a pole).

All of this to say that with $K_i \geq 0$, conditions (21) and (22) of passivity are always verified for Y_{rh}, Y_{rt} and Y_{ah}. Therefore the last condition of passivity (23) is necessary and sufficient for proving passivity in our system. Consequently (40) is a necessary an sufficient condition for UCS with limited tool inertia.

C. Gain domain

We already have $K_i \geq 0$. In order to better understand the limitations introduced by the criteria 'UCS with limited load inertia' (41 to 44), we will express the controler gain bounds in case of our simplified flexible robot model, thus $B_t = T_c = T_{cv} = 0$ in (14) and (15).

It is possible to express the conditions for 'UCS with limited load inertia' (41 - 44) as a ratio of two polynomial expressions in ω^2, with a positive denominator. Thus we just have to check that the numerator is positive for $\omega \in \mathbb{R}$. Except for condition (42), the numerator polynomials are of 1st order. After this calculus step with obtain the following bounds: (41), is equivalent to :

$$\frac{K_i.K_v}{K_v + B_m} \leq \frac{K_{ph}.K_v + 1}{J_r + J_m} \tag{53}$$

$$\frac{K_i.K_v}{K_v + B_m} \geq \frac{K_{ph}}{K_v.J_m} \tag{54}$$

(43), is equivalent to :

$$\frac{K_i.K_v}{K_v + B_m} \geq \frac{K_{ph} - K_{pt}}{Kv.J_m.(1-\gamma)} \tag{55}$$

$$\gamma.K_{ph} - K_{pt} \leq \frac{1-\gamma}{K_v} \tag{56}$$

(44), is equivalent to :

$$\frac{K_i.K_v}{K_v+B_m} \leq \frac{K_{ph}.K_v+1}{J_r+J_m+J_{tmax}.(1-\gamma+K_v.(K_{ph}-\gamma.K_{pt}))} \quad (57)$$

$$\frac{K_i.K_v}{K_v+B_m} \leq \frac{K_v.K_{ph}.(J_r+J_{tmax})-K_{pt}.J_{tmax}}{J_m.(J_r+J_{tmax}.(1-\gamma))} \quad (58)$$

D. Limitation on Robot minimum inertia

When the operator moves the robot quickly and/or repeatedly from one position to another using its end-effector handle, he will feel that the robot behaves like a pure inertia. We may define the load-free appearing inertia of the robot on the operator port J_{rh} as :

$$\begin{aligned} \omega \to 0 \Rightarrow Y_{rh}(s) &\approx \frac{1}{J_{rh}.s} \\ \Rightarrow J_{rh} = \lim_{s\to 0} \frac{1}{s.Y_{rh}(s)} &= \frac{1}{K_i.\alpha(0)} \end{aligned} \quad (59)$$

In order to limit operator fatigue in free movements, we want J_{rh} to be as low as possible. Substituting (50) in (59) we obtain :

$$J_{rh} = \frac{K_v+B_m}{K_v.K_i} \quad (60)$$

Combining (54), (55) and (58) conditions on the controller gains, we found that necessarily (60) cannot be lower than :

$$J_{rh} \geq J_r + (1-\gamma).J_{tmax} \quad (61)$$

Futhermore, to achieve the minimal inertia this imply taking :

$$K_{pt} = K_{ph}.\gamma. \quad (62)$$

We can also define J_{rt}, the appearing controlled robot inertia at the tool port. (6) implies that :

$$J_{rt} = \frac{J_{rh}}{\gamma} \quad (63)$$

It can be seen that the inertia at the tool port J_{rt} can be very important for high force augmentation ratio ($\gamma \to 0$). This could be unsecure/dangerous if the operator unwillingly drops its handle during a fast movement. This would result in a potentially dangerous tool (a sharp blade in our example) moving freely at high speed with high inertia.
This issue may be avoided for example using a pressure sensitive handle, and scheduling the amplification ratio on its pressure measurement, in order to achieve $\gamma = 1$ (thus minimal tool inertia) when the handle is dropped (no pressure detected on the handle).

E. Sensor bandwidth limitations

We will now take into account the effect of damping in the robot flexibility ($B_t > 0$), the limited bandwidth of the force sensors ($T_c > 0$) and the limited bandwidth of the velocity measurement ($T_{cv} > 0$). In order to achieve minimum inertia on the operator side we will satisfy (62). In order to draw the possible (K_i, K_{ph}) gain region, that satisfie UCS with limited inertia conditions (41 to 44) we numerically verified thoses conditions for every gains using 10000 logarithmically distributed points on the frequency range from 0.1Hz to 1kHz.
Unfortunately we found that condition (43) was not completly verified for some frequency, although it was easy to satisfy in our simple flexible model (55) and (56). Therefore instead we used the UCS with limited inertia and stiffness criteria. With:

$$\begin{aligned} J_{tmax} &= 6.0 \quad kg.m^2.rad^{-1} \\ K_{tmax} &= 6.7e5 \quad N.m.rad^{-1} \end{aligned}$$

Note that here we allow a much stiffer tool contact than the robot own siffness K_t, therefore in pratice it should not be very limitating if we have to use a mechanical filter between the tool and the robot. On fig. 9 is drawn the resulting computed (K_i, K_{ph}) allowable gain region.

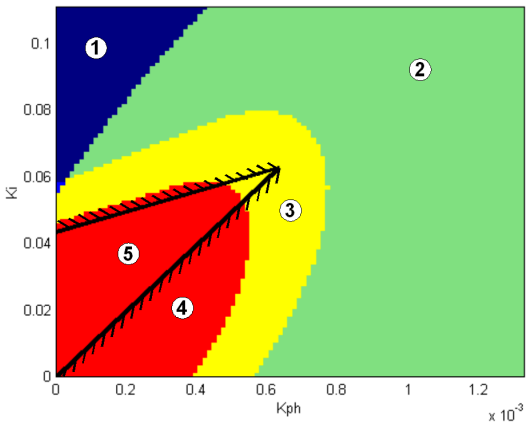

Fig. 9. This figure shows the gains domain where the conditions for UCS with limited tool inertia and stiffness are met when considering the full model. In area 1 only condition (42) is satisfied. In area 2, only condition (46) is met. In area 3, conditions (46) and (41) are met. In area 4 all conditions are fullfilled (41,42,46 and 44). Area 5 which is delimited by the black lines is the same as 4 but considering the simplified model.

V. Experimental results

In order to compare our theoretical result to the real example we realized experiements on a RX90 robot from Stäubli. the presented control loop of fig. 4 has been implemented on the real time operation system VxWorks. The sampling period is $3\,ms$. The both force/torque sensors used are ATI sensors.

A. Pure spring as operator impedance experiment

In order to check the passivity on the operator port, we attach the handle to a rigid wall through a spring of stiffness around $3500\,N.rad^{-1}$. This represent a chalenging operator impedance Z_h for passivity, because it almost doesn't disipate any energy. On fig. 10 we tried different combinaisons of K_i and K_{ph}, if the system get unstable then we are sure that the controller is not passive for this setting.

We can see from those experiements that the upper domain bound is overestimated of about 10%. Unfortunatly we were

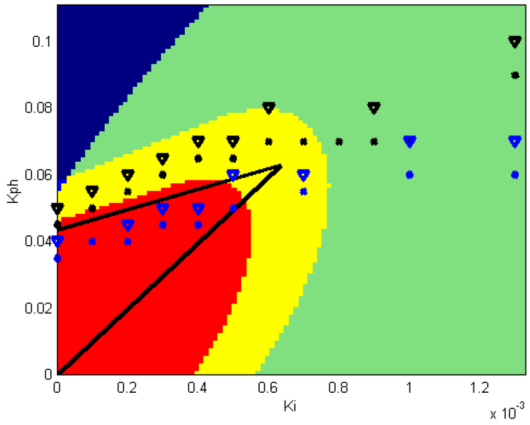

Fig. 10. On the theoretical gain domain, we have plotted the results of the experiments we conducted to challenge passivity. The operator handle was attached to a wall through a spring. Black signs correspond to experiments with tool port unconnected. Blue signs correspond to experiments with tool port connected to the maximum allowed tool inertia. Triangle means that the system was unstable. Dots means that the system was stable

not able to observe the lower/rigth border with this experiment, because the corresponding environment impedance did not cover that domain : a stiffer spring should be used.

B. Force bandwidth against stiff environnement

In order to evaluate the resulting force amplification bandwidth, we asked an operator to push on the robot handle in order to make the tool apply an high force on the wall. In this experiment, the tool inertia was about half J_{tmax}. We can see the result on fig. 11.

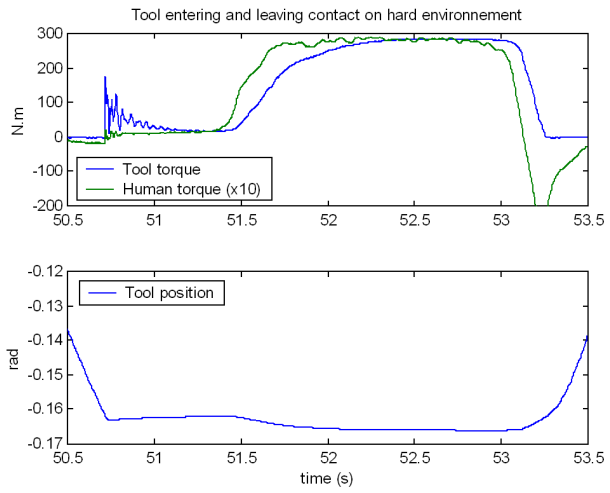

Fig. 11. The 10x force amplification control is implemented. The operator is asked to move the handle in order to make the tool apply force on a stiff wall. Very High Transitional forces are not felt by the operator when contact occur, and also a sticky effect is felt when user quickly wants to remove the tool. When tool is moving in free space, its torque is null.

The system behaves safely. First the user makes the robot enter in contact. The contact is established at $t = 50.7$ with little vibrations that are not felt by the user and smoothly stabilized within about half a second. Then the user starts to apply an higher force at $t = 51.5$, the torque on tool side rise up to 10 times the operator applied force with a delay about a quater of second. This delay is due to the integrator contribution. The same delay is observed when the operator starts to remove the contact at $t = 53.2$. A sicky effect is felt by the operator at this time.

This experiment suggeste that the bandwidth limitation could also be an important performance criterion that should be tuned using another relationship between K_{ph} and K_{pt}, different from (62).

VI. Conclusions and Future Work

We have successfully implemented a force amplification control on an industrial robot and derived its dynamic limitations. This leads to a new result: the minimum achievable inertia of respectively the handle and the tool depends on the chosen amplification factor and the physical caracteristics of the robots that have been modeled and identified in order to set the control gains of the controller.

Interestingly, the proposed controller is proven passive for a set of bounded load inertia and environment stiffness. Experiments emphasized great robustness with acceptable performances with little vibrations smoothly stabilized.

The next step of our work, will be to optimize also the force augmentation bandwidth against stiff environnement. Afterwhile we will have to consider expanding this study to the five remaining DoFs of the robot.

References

[1] K. Kosuge, Y. Fujisawa, and T. Fukuda, "Control of robot directly maneuvered by operator," 1993, pp. 49–54 vol.1.

[2] J. Colgate, M. Peshkin, and S. Klostermeyer, "Intelligent assist devices in industrial applications: a review," in *Intelligent Robots and Systems, 2003. (IROS 2003). Proceedings. 2003 IEEE/RSJ International Conference on*, vol. 3, 2003, pp. 2516–2521 vol.3.

[3] K. Lee, S. Lee, J. Choi, S. Lee, and C. Han, "The application of the human-robot cooperative system for construction robot manipulating and installing heavy materials," in *SICE-ICASE, 2006. International Joint Conference*, 2006, pp. 4798–4802.

[4] X. Lamy, F. Colledani, F. Geffard, Y. Measson, and G. Morel, "Robotic skin structure and performances for industrial robot comanipulation," in *Advanced Intelligent Mechatronics, 2009. AIM 2009. IEEE/ASME International Conference on*, 2009, pp. 427–432.

[5] W. S. Newman and Y. Zhang, "Stable interaction control and coulomb friction compensation using natural admittance control," *Journal of Robotic Systems*, vol. 11, pp. 3–11, 1994.

[6] B. Cagneau, G. Morel, D. Bellot, N. Zemiti, and G. d'Agostino, "A passive force amplifier," in *Robotics and Automation, 2008. ICRA 2008. IEEE International Conference on*, 2008, pp. 2079–2084.

[7] X. Lamy, F. Colledani, F. Geffard, Y. Measson, and G. Morel, "Achieving efficient and stable comanipulation through adaptation to changes in human arm impedance," in *Robotics and Automation, 2009. ICRA '09. IEEE International Conference on*, 2009, pp. 265–271.

[8] J. E. Colgate and N. Hogan, "Robust control of dynamically interacting systems," *International Journal of Control*, vol. 48, pp. 65 – 88, July 1988, department of Mechanical Engineering, Massachusetts Institute of Technology, Cambridge, MA, U.S.A.

[9] J. Dolan, M. Friedman, and M. Nagurka, "Dynamic and loaded impedance components in the maintenance of human arm posture," *Systems, Man and Cybernetics, IEEE Transactions on*, vol. 23, pp. 698–709, 1993.